DYNAMICS OF ELECTROMECHANICAL DRIVE OF SUSPENDED TIMBERTRANSPORTING ROPE SYSTEM

Lidiya Dzyuba[1], Vasyl Baryliak[2]

[1] Department of Applied Mathematics and Mechanics, Lviv State University of Life Safety, Ukraine
[2] Department of Applied Mechanics, Ukrainian National Forestry University, Lviv, Ukraine

A b s t r a c t

Dynamic loads of drive of suspended timbertransporting rope system with an electric motor are investigated. Developed a dynamic model of the electromechanical drive considering the changing of the electric motor's moment during start-up and the resistance force moment. The changing of the resistance force moment is expressed through the changes in tension force of the pull-bearing rope systems in various manufacturing operations. In determining the moment of inertia of the drive drum is accounted multi-winding of rope. Research on dynamic load of system elements are made with the taking into account the influence of torsional stiffness of system parts and lifting capacity of the suspended timbertransporting rope system.

Introduction

The suspended timbertransporting rope systems have a number of advantages for the primary transportation of timber in mountainous areas compared with tractor skidding. Such as: much lower amount of roads building, the use in any weather and at any soils, waste reduction at cutting areas, the possibility of exploration of forests in inaccessible places for other equipment, reducing energy costs and protecting the environment (ADAMOVSKY et al. 1997, BELAYA, PROHORENKO 1964, KORZHOV, CUDRA 2010). These systems are equip-

Correspondence: Vasyl Baryliak, Ukrainian National Forestry University, Lviv, Ukraine, e-mail: barylyakw@gmail.com
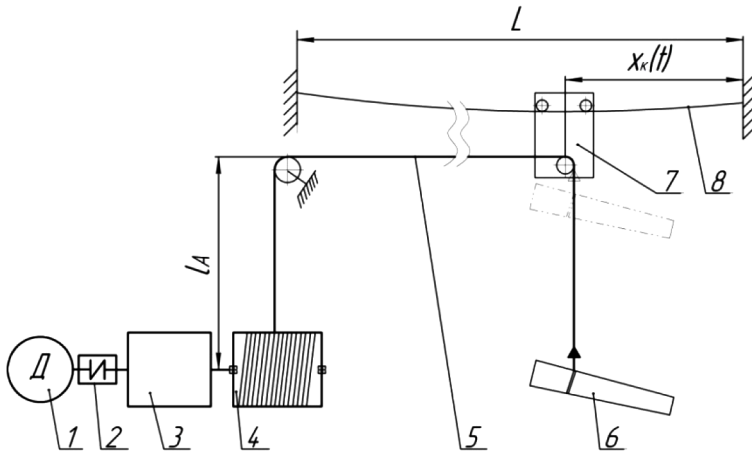
Fig. 1. Schematic diagram of one-drum drive of the timbertransporting rope system: *1* – electric motor; *2* – coupling; *3* – mechanical transmission; *4* – drive drum of power stroke; *5* – pull-hoisting rope; *6* – load; *7* – load carriage; *8* – carrier rope; – span length of the rope system; $x(t)$ – coordinate of load carriage in the span; l_A – length of the reserve rope

ped with electric motor drives or an internal combustion engine (ZANEHYN et al. 2004). The characteristic features of the system drive's work are variable tension force of pull-hoisting rope by various manufacturing operations and multi-winding of rope on the drum. The change of the pull-hoisting rope's tension causes the change of force resistance moment at different stages of the system's process (MALASHHENKO et al. 2013). The multi-winding of the drum drive rope increases its diameter with the wound rope. It causes the changing of the inertia moment of the drive drum. The presence of the drive electric motor causes bigger dynamic loads on system elements when the system is turning on (CZABAN 2008, CZABAN, LIS 2012, KHARCHENKO, SOBKOWSKI 2005). The suspended timbertransporting rope systems are characterized by a low level of unification schemes and constructions. Therefore, the proposed model needs detailing of considering operational and structural features.

The objective is the mathematical modeling of dynamic processes of the suspended timbertransporting rope system's drive with taking into account the changing of the electric motor's moment during start-up and the resistance moment during a steady-state operation mode of the system and studying the impact of structural and operational parameters on the value of dynamic loads in the drive.

To achieve this goal it is necessary to develop a dynamic model of the rope system's drive and take into account, in addition to inertial, elastic and dissipative characteristics of parts, multi-layer winding rope and the real nature of changes in external loads.

Theoretical research

One-drum drive of the timbertransporting rope system is simulated as the equivalent reduced tri-mass dynamic system with three degrees of freedom (Fig. 2). The motor shaft is used as a section of reduction.

Differential equations of drive's motion write down using the principle of d'Alembert in the normal form of Cauchy:

$$
\begin{cases}
\dfrac{d\varphi_1}{dt} = \omega_1 \\[2mm]
\dfrac{d\varphi_2}{dt} = \omega_2 \\[2mm]
\dfrac{d\varphi_3}{dt} = \omega_3 \\[2mm]
\dfrac{d\varphi_1}{dt} = \dfrac{1}{I_1} \cdot [M_E - v_1(\omega_1 - \omega_2) - c_1(\varphi_1 - \varphi_2)] \\[2mm]
\dfrac{d\varphi_2}{dt} = \dfrac{1}{I_2} \cdot [v_1(\omega_1 + \omega_2) - c_1(\varphi_1 - \varphi_2) - v_2(\omega_2 + \omega_3) - c_2(\varphi_2 - \varphi_3)] \\[2mm]
\dfrac{d\varphi_3}{dt} = \dfrac{1}{I_3(t)} \cdot \left[-M_S(t) - \dfrac{\omega_3}{2}\dfrac{d[I_3(t)]}{dt} + v_2(\omega_2 + \omega_3) - c_2(\varphi_2 - \varphi_3)\right]
\end{cases}
\tag{1}
$$

where:
ω_1, ω_2, ω_3 – angular velocity of corresponding reduced rotating masses, t – time.
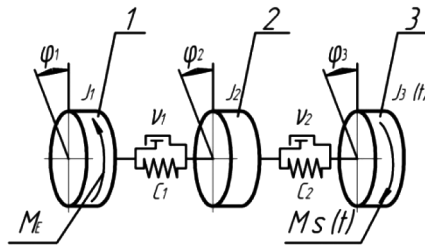

Fig. 2. Estimated diagram of the one-drum drive of the timbertransporting rope system
The notation used on Fig. 2: *1* – rotating mass of motor's rotor and coupling; *2* – reduced rotating mass of drive's mechanical transmission; *3* – reduced rotating mass of drive's drum, pull-hoisting rope and transported load with the load carriage; M_E – electromagnetic moment of motor; $M_S(t)$ – resistance force moment of the drum drive with traction rope reduced to the motor shaft; I_1 – inertia moment of the rotating masses of motor and coupling; I_2 – inertia moment of the drive's mechanical transmission reduced to the motor shaft; $I_3(t)$ – inertia moment of the rotating mass is equivalent to the masses of drive drum, pull-hoisting rope, load with the load carriage and reduced to the motor shaft; c_1, c_2 – reduced coefficients of torsion stiffness of elastic sections; v_1, v_2 – reduced coefficients of elastic sections' viscous resistance; φ_1, φ_2, φ_3 – generalized coordinates of drive's rotating masses.

The transient electromagnetic processes in the drive asynchronous electric motor with a shortcircuited rotor (squirrel cage motor) is described briefly based on Park-Gorev equations (PARK 1929, PARK 1933, GOREV 1950). Electromagnetic moment of motor M_E is calculated using the formula (KHARCHENKO, SOBKOWSKI 2005, JOSWIG 2014):

$$M_E = \frac{2}{3}\, p_0\, \frac{1}{\tau}\, (i_{Rx} i_{Sy} - i_{Ry} i_{Sx}) \tag{2}$$

where:
p_0 – the number of pairs of magnetic poles; $i_{Rx}, i_{Sy}, i_{Ry}, i_{Sx}$ – the projections of currents in the windings of the motor's stator and rotor on the coordinate axes x, y ; τ – the value, which is determined from the magnetization curve. Subscript indicates the value of belonging to the rotor winding, a S – indicates the value of belonging to the stator winding.

The projections of currents $i_{Rx}, i_{Sy}, i_{Ry}, i_{Sx}$ are determined from differential equations of the electromagnetic state of machines (CZABAN 2007, CZABAN, LIS 2012, JOSWIG 2014, KHARCHENKO, SOBKOWSKI 2005), that are written down in matrix form:

$$\frac{di_S}{dt} = A_S(u_S + \Omega_S \psi_S - R_S i_S) + B_S(\Omega_R \psi_R - R_R i_R)$$

$$\frac{di_R}{dt} = A_R(\Omega_R \psi_R - R_R i_R) + B_R(u_S + \Omega_S \psi_S - R_S i_S) \tag{3}$$

where:
i_S, i_R, u_S – *matrices column of currents and voltages;* A_S, B_S, A_R, B_R – square matrices of communication; Ω_S, Ω_R – frequency rotation matrices; ψ_S, ψ_R – matrices-column of full flows clutches; R_S, R_R – active resistance.

The reduced resistance force moment $M_S(t)$ determine, taking into account the variable of tension force of pull- hoisting rope $S(t)$ and variable radius $r_H(t)$ and variable radius of the drum with wounded rope:

$$M_S(t) = \frac{1}{u}\, S(t) \cdot r_H(t) \tag{4}$$

where:
u – general gear ratio of drive's mechanical transmission.

To determine the tension force $S(t)$ the technological cycle of work of suspended timbertransporting rope system will be examined. It is divided into the following four stages:

– selection of rope's weaknesses (characterized by a progressive increase of tension force of the rope to a value equal to the weight of cargo);

– lifting cargo;

– locking cargo with the load carriage;

– transferring cargo with the load carriage along the rope.

The pull-tension power of hoisting rope is determined considering the location coordinates of load carriage, rope system's process parameters and the duration of each of the stages according to the steps of technological cycle (ADAMOVSKY et al. 1997, ZANEHYN et al. 2004):

$$S(t) = \begin{cases} 0 \le t \le \dfrac{Q[L - x_K(t_0)]}{C_K \cdot v} \Rightarrow S_0(t) = \dfrac{C_K \cdot v}{L - x_K(t_0)} \cdot t \\[2ex] \dfrac{Q[L - x_K(t_0)]}{C_K \cdot v} < t \le \dfrac{1}{v}\left(\dfrac{Q[L - x_K(t_0)]}{C_K} + H_G\right) \Rightarrow S_1(t) \\[2ex] \left[\dfrac{1}{v}\left(\dfrac{Q[L - x_K(t_0)]}{C_K} + H_G\right) < t \le \dfrac{1}{v}\left(\dfrac{Q[L - x_K(t_0)]}{C_K} + H_G\right) + t_C\right] \Rightarrow S_2(t) \\[2ex] \left.\begin{array}{l} t > \dfrac{1}{v}\left(\dfrac{Q[L - x_K(t_0)]}{C_K} + H_G\right) + t_C \\[2ex] t \le \dfrac{1}{v}\left(\dfrac{Q[L - x_K(t_0)]}{C_K} + H_G\right) + \dfrac{L - x_K(t_0)}{\cos\beta} + \dfrac{(gq_K)^2 \cdot (L - x_K(t_0))^3}{24 \cdot H^2}\cos\beta\right) + t_C \end{array}\right\} \Rightarrow S_3(t) \end{cases} \quad (5)$$

where:

$S_0(t)$, $S_1(t)$, $S_2(t)$, $S_3(t)$ – pull-tension power of hoisting rope when choosing rope's weaknesses, lifting cargo, locking cargo with the cargo carriage and transporting of cargo carriage by carrier rope (ADAMOVSKY et al. 1997, ZANEHYN et al. 2004), Q – cargo weight; $x_K(t_0)$ – coordinate of cargo carriage at the initial time t_0; H_G – height of lifting cargo; v – velocity of winding of rope on the drum; β – angle between the span's chord and the horizon; C_K – longitudinal stiffness of pull-hoisting rope; – horizontal component of the tension force of the rope (ADAMOVSKY et al. 1997, BELAYA, PROHORENKO 1964, ZANEHYN et al. 2004); t_C – time of cargo's locking (ADAMOVSKY et al. 1997); q_K – mass per unit length of the rope.

The expression for determining the radius of the drum with wounded rope in the random time moment writes down as follows:

$$r_H(t) = \frac{d_{B3}}{2} + d_K \cdot (n^/(t) - 0{,}5), \qquad (6)$$

where:

d_{B3} – diameter of the drum without a rope, d_K – rope's diameter, $n^/(t)$ – the number of wound rope's layers.

To determine $n^/(t)$, express estimated number of wound rope's layers through the angular rotation velocity of the drum drive:

$$n(t) = n_0 + \frac{\omega_{B3}(t) \cdot d_K \cdot t}{2\pi L_{B3}}, \qquad (7)$$

where:
$n(t)$ – angular velocity of the drum drive with rope; n_0 – the number of wound rope's layers at the initial time moment t_0; L_{B3} – length of the working surface of the drum. To get the value of $n^/(t)$ round the value of $n(t)$ to the upper whole number.

To determine the value of n_0 is used known dependency for the length of wound rope on the drum (GOROKHOVSKI, LIVSHITS 1991):

$$l_0 = \pi \cdot \frac{L_{B3}}{d_K} \cdot n_0 \cdot [d_{B3} + C_y \, d_K \cdot (n_0 - 1)] \qquad (8)$$

where:
C_y – the ratio of wound rope's density.

The length of wound rope at the initial time moment is determined because total capacity of the rope of the drum drive and coordinate's placement of cargo carriage in flight are set. Taking into account the rope's sagging by a parabola (ADAMOVSKY et al. 1997, BELAYA, PROHORENKO 1964) and the available rope's reserve (GOROKHOVSKI, LIVSHITS 1991, KORZHOV, CUDRA, 2010) this length is equal to:

$$l_0 = l_A + \frac{x_K(t_0)}{\cos\beta} + \frac{q_K^2 \cdot x_K(t_0)^3}{24H^2} \cos\beta \qquad (9)$$

Equating (8) and (9), we obtain an expression for determining the number of wound rope's layers at the initial time t_0:

$$n_0 = \frac{C_y d_K - d_{B3} + \sqrt{(d_{B3} - C_y d_K)^2 + \dfrac{4C_y d_K^2 l_0}{\pi \cdot L_{B3}}}}{2C_y d_K} \qquad (10)$$

Thus, the radius of the drum with wounded rope at a random moment of time is calculated by the relation (6) using (7) – (10).

To determine the variable reduced moment of $I_3(t)$ specified stages of the rope system's cycle of work must be taken into account. The inertia moment of of the drive drum, the mass of cargo and area of rolling rope are forming factors for $I_3(t)$ at the stage of lifting and locking loads. The expression for determining the reduced moment of inertia at this stage is:

$$I_3(t) = \frac{1}{u^2}\left(I_{B3}(t) + \frac{q_K}{3}\left(\frac{L - x_K(t_0)}{\cos\beta} + \frac{q_K^2 \cdot (L - x_K(t_0))^3}{24H^2}\cos\beta\right)r_H^2(t) + \frac{Q}{g}r_H^2(t)\right)$$

(11)

where:
u – general gear ratio of drive's transmissions; I_{B3} – inertia moment of the drive of the drum.

To determine the reduced moment $I_3(t)$ the moving mass of cargo carriage is taken to account at the stage of displacement:

$$I_3(t) = \frac{1}{u^2}\left(I_{B3}(t) + \frac{q_K}{3}\left(\frac{L - x_K(t_0)}{\cos\beta} + \frac{q_K^2 \cdot (L - x_K(t_0))^3}{24H^2}\cos\beta\right)r_H^2(t) + \frac{Q + G}{g}r_H^2(t)\right)$$

(12)

where:
G – weight of cargo carriage.

The drive drum's moment of inertia depends on the drum's weight with the wound rope and the distribution of mass in the drum (ADAMOVSKY et al. 1997, MALASHHENKO et al. 2013):

$$I_{B3}(t) = k_M \cdot [m_{B3} + l_T(t) \cdot q_K] \cdot r_H^2(t),$$

(13)

where:
k_M – coefficient of mass distribution in the drum ($k_M = 0,7$); m_B – mass of drive drum without a rope; $m_K(t)$, $l_T(t)$ - mass and length of wound rope.

The length of wound rope at the initial time moment is is determined by taking into account (7):

$$l_T(t) = \pi \cdot \frac{L_{B3}}{d_K} \cdot n_0 + \frac{\omega_{B3}(t)\cdot d_K \cdot t}{2\pi L_{B3}} \cdot \left[d_{B3} + C_y \cdot d_K \cdot \left(n_0 + \frac{\omega_{B3}(t) \cdot d_K \cdot t}{2\pi L_{B3}} - 1\right)\right].$$

(14)

Taking into account (13), (14) the expression (11), (12) can calculate a reduced moment of inertia $I_3(t)$.

Results and discussion

Since all the drum's elements are fixed at the time of motor's start-up, all the angles of rotation φ_i and angular velocity ω_i of reduced masses are equal to zero.

The value of the currents in the windings of the motor at the initial start-up time are equal to zero, and therefore the projection of these currents on the coordinate axes are also equal to zero. Thus, there are zero initial conditions at the initial time t_0:

$$t_0 = 0,\, i_{Sx}(t_0) = 0,\, i_{Sy}(t_0) = 0,\, i_{Rx}(t_0) = 0,\, i_{Ry}(t_0) = 0,\, \varphi_1(t_0) = 0,\, \varphi_2(t_0) = 0,\, \varphi_3(t_0) = 0,$$
$$\omega_1(t_0) = 0,\, \omega_2(t_0) = 0,\, \omega_3(t_0) = 0.$$

The differential equations (1) and (3) with given initial conditions form a closed system that describes the dynamic state of the electromechanical drive. It is solved by Euler's numerical method with recalculation. At each step, common numerical integration of differential equations (1) and (3) determine the drive's variables:

– electromagnetic moment of the motor M_E;

– reduced moment of the force resistance on the drive drum $M_S(t)$;

– increasing of the dynamic moment due to increasing the moment of inertia of the drum drive $\dfrac{d[I_3(t)]}{dt}$.

The solution of systems of differential equations (1) and (3) allows determining the parameters of the motion of drive's mechanical part such as rotating angles and angular velocities of reduced rotating masses. In addition to the motion parameters of the mechanical part, you can also define the electromagnetic moment and angular velocity of the motor's rotor. The time dependencies of reduced dynamic moments in the parts of drive's dynamic model can be build using determined motion parameters.

The reduced dynamic moments in the drive's coupling and mechanical transmissions are calculated as follows:

– the reduced dynamic moments in the drive's coupling:

$$M_{d1} = c_1[\varphi_1 - \varphi_2] + v_1[\omega_1 - \omega_2] \tag{15}$$

– the reduced dynamic moments in the drive's mechanical transmissions:

$$M_{d2} = c_2[\varphi_2 - \varphi_3] + v_1[\omega_2 - \omega_3] \tag{16}$$
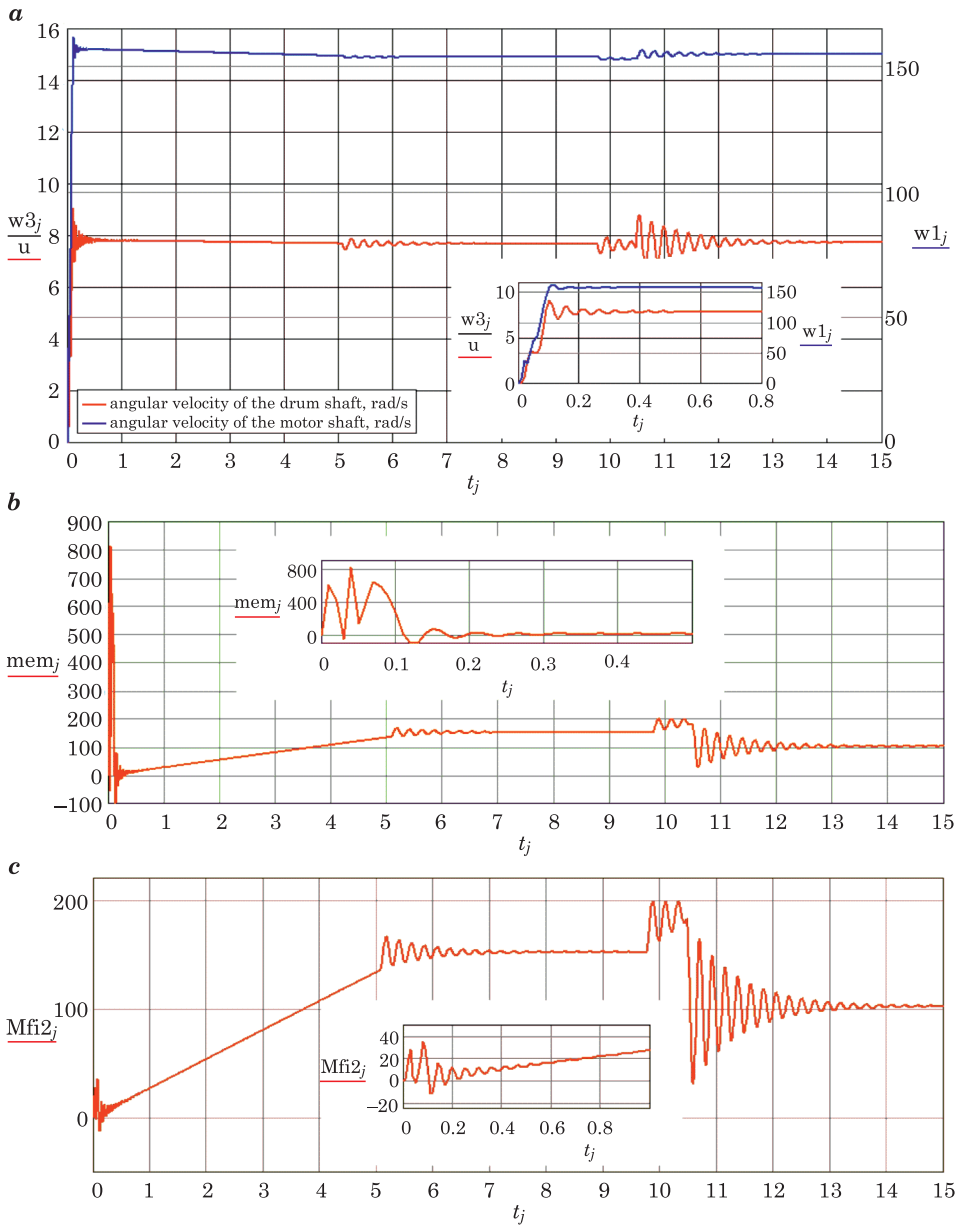
a

b

c

Fig. 3. The time dependence of the angular velocity drive's shaft (a) of the electric motor's moment (b) and reduced dynamic moment in drive's transmissions (c).

The example of calculating the angular velocity and dynamic moments in one-drum drive equipped with an electric motor and elastic coupling shown in Fig. 3-4 in graphs. The calculation is performed using the following inputs:

electric motor 4A180M4 (R_S = 0,134 Om; R_R = 0,117 Om; L_S $^{=\ 0,8\ \cdot\ 10^{-3}}$H; L_R = 0,82 · 10^{-3}H; L_m = 4,9 · 10^{-2}H; U_m = 310,5 W; α_1 = 4,714 · 10^{-2} Wb/A; α^2 = –2,094 · 10^{-5} Wb/A^3; α_3 = 6,003 · 10^{-9} Wb/A^5; i_{mk} = 15,0 A; ω_0 = 157 rad/s; p_0 = 2); J_1 = 23,5 kg/m^2; J_2 = 0,02 kg/m^2; c_1 = 35*10^3N*m/rad; c_t = 40*10^3N*m/rad; v_1 = 15N*m*s/rad; v_2 = 2,96*10^{-3}N*m*s/rad; L = 400m; $x_K(t)$ = 80 m; Q = 16 kH; G = 240 N; u = 20; H_G = 4 m; m_{B3} = 30 kg; L_{B3} = 0,6 m; d_{B3} = 0,3 m; d_K = 9,7 · 10^{-3} m; β = 30º.

The analysis of graphs has shown that acceleration of drive system is less than 0.2 s (Fig. 3a). The initial phase of acceleration accompanied by intense electromagnetic fluctuations of the electric motor (800) with a frequency of power line 50 Hz (Fig. 3b). This small acceleration time due to the lack of technological load at the time of start and a gradual linear increase of tension force of pull- hoisting rope at the initial of the technological cycle from zero to a value of . The amplitude and intensity fluctuations of reduced dynamic moment in transferring (Fig 3c) during start-up is much lower (up to 40N*m). Low values of amplitude and intensity fluctuations of dynamic moments in transmissions drive during acceleration is also due to the linear nature of the increasing process of load and reducing the influence of fluctuations of the electric motor to the transmission due to the elastic properties of the coupling.

During the separation of load bearing surface (5.5–6.5 second of work) and docking with the cargo load carriage (9.5 seconds of work) observed synchronous oscillation of angular velocities of the drive shaft of the electric motor and the drive drum (Fig. 3a). The amplitude of oscillation of the angular velocity of the motor shaft is higher than during start-up. The dynamic moment in the line of drive's transmissions (Fig. 3b) also reaches maximum values (up to 230) during the separation of load bearing surface and with locking the cargo freight carriage.

Therefore, the start-up and acceleration stage of transmissions drive are less dangerous compared to locking cargo and cargo separation from the bearing surface.

To evaluate the dynamic loads of the drive the coefficient of dynamics k_d is used:

$$k_d = \frac{M_{d\,\max}}{M_n} \qquad (17)$$

where:

$M_{d\,\max}$ – maximum value of reduced dynamic moment in mechanical transmissions drive, calculated by the formula (16); M_n – elevated moment at the nominal load. The value of cargo is used as the nominal load. Reduced to the motor shaft moment from the nominal load is calculated as follows:

$$\mathrm{M_n} = \frac{Q \cdot r_H^/(t)}{u} \tag{18}$$

where:

$r_H^/(t)$ – radius of the drive drum with wound rope at the time of action of maximum dynamic load in the transmissions drive.

The reduced coefficient of torsion stiffness is an important generalized indicator that considers both the geometric dimensions and mechanical characteristics of the material of the drive parts and kinematic characteristics (the gear ratio of drive mechanical transmission). Therefore, the limits for the selection of values of reduced torsion stiffness coefficient, when the dynamic load factor will be of the smallest values are substantiated in the article. The calculation of dynamic coefficient performed for different values of cargo weight and reduced torsion stiffness coefficients of drive's units (Fig. 4).
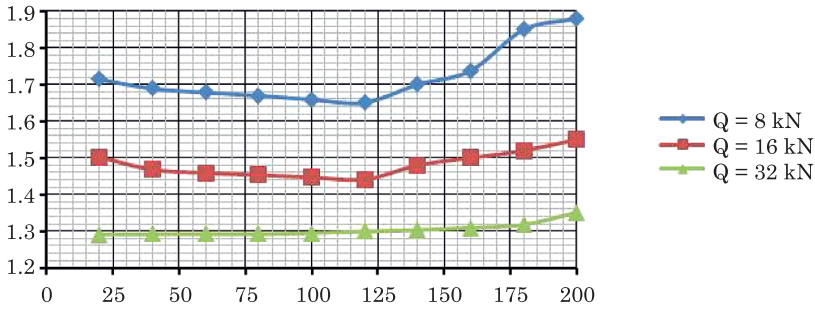

Fig. 4. Graphs of the dependence of dynamic coefficient on reduced coefficient of torsion stiffness transmissions of the one-drum drive of the timbertransporting rope system.

Conclusions

1. Studies have shown the most potentially dangerous operating modes of timbertransporting rope system are periods of separation of cargo's bearing surface and locking of cargo with cargo carriage. At higher values of cargo weight (Q = 32..64 kN) the more dangerous mode is a time of separation of cargo from bearing surface, and at lower values of cargo weight (Q = 8..16 kN) – the process of locking cargo with cargo carriage.

2. The dynamic load is minimal and close to a constant value in the range of reduced coefficients of the torsion stiffness of transmissions of 100 ... 125 N*m/rad. Therefore, geometric and kinematic parameters of mechanical transmissions and shaft drive of timbertransporting rope systems are recommended to have its reduced torsional stiffness transmissions coefficient between indicated limits.

References

ADAMOVSKY M., MARTYNTSIV M., BADERA J. 1997. *Suspended cable timbertransporting plants*, IZMN, Kyiv.

BARYLIAK V. 2015. *Justification of the parameters of the drives of timber transporting rope systems.* Dissertation for the degree of the Candidate of engineering science (comparable to the academic degree of Ph.D.), Lviv.

BELAYA N., PROHORENKO A. 1964. *Cable timbertransporting plants,* Forest Industry, Moscow.

CZABAN A. 2007. *Mathematical modeling of processes oscillating electromechanical systems,* T. Soroki, Lviv.

CZABAN A., LIS M. 2012. *Mathematical modelling of transient states in a drive system with a long elastic element. Electrical Review.* R. 88, nr 12b, (pp. 167–170), Sigma-Not, Warsaw.

GOREV A.A. 1950. *The transient processes of synchronous machine.* Moscow.

GOROKHOVSKI K., LIVSHITS N. 1991. *Machines and equipment for logging and forest storage works.* Ecology, Moscow.

JOSWIG Fr. 2014. *The electro-mechanical coupling as the cause of torsional oscillations and their effects on shafting.* Dissertation for the academic degree Doctor of Engineering. Dortmund.

KHARCHENKO YE., SOBKOWSKI S. 2005. *Mathematical modelling of transients in drives of building elevating devices , Diagnostyka. Quarterly published by the Polish Society of Technical Diagnostics.* Vol. 35, (pp. 37–42), Warsaw.

KORZHOV V., CUDRA V. 2010. *Constructive-technological features of mobile cable timbertransporting plants of built up type. Industrial hydraulics and automation.* Vol. 3.29, (pp. 18–20). Lviv.

MALASHHENKO V., MARTYNCIV M., BARYLIAK V. 2013. *Research of work of cable timber transporting plants drives with regard multilayer winding rope. Lifting and conveying equipment.* 2, (pp. 29–38), Dnipropetrovsk.

PARK R.H. 1929. *Two-reaction theory of synchronous machines generalized method of analysis-part I. Transactions of the American Institute of Electrical Engineers.* Vol. 48, (pp. 716–727), (republished NAPS, University of Waterloo, Canada. 2000), Waterloo.

PARK R.H. 1933. Two-reaction theory of synchronous machines -part II. *Transactions of the American Institute of Electrical Engineers.* Vol. 52, (pp. 352–354).

ZANEHYN L., VOSKOBOINIKOV I., YEREMEEV N. 2004. *Machines and Mechanisms for cable logging.* MHUL, Moscow.